Zhi-Chao Feng,[1,2] Alex Popell,[1,2] Jinming Li,[1,2] Jenna Silverstein,[1,2] Amanda Oakie,[1,3] Siu-Pok Yee,[4] and Rennian Wang[1,2,5]

c-Kit Receptor Signaling Regulates Islet Vasculature, β-Cell Survival, and Function In Vivo

Diabetes 2015;64:3852–3866 | DOI: 10.2337/db15-0054

The receptor tyrosine kinase c-Kit plays an integral role in maintaining β-cell mass and function. Although c-Kit receptor signaling promotes angiogenesis in multiple cell types, its role in islet vasculature is unknown. This study examines the effects of c-Kit–mediated vascular endothelial growth factor isoform A (VEGF-A) and islet vascularization on β-cell function and survival using in vitro cell culture and in vivo mouse models. In cultured INS-1 cells and primary islets, c-Kit regulates VEGF-A expression via the Akt/mammalian target of rapamycin (mTOR) signaling pathway. Juvenile mice with mutated c-Kit (*c-Kit*$^{Wv/+}$) showed impaired islet vasculature and β-cell dysfunction, while restoring c-Kit expression in β-cells of *c-Kit*$^{Wv/+}$ mice rescued islet vascular defects through modulation of the Akt/mTOR/VEGF-A pathway, indicating that c-Kit signaling in β-cells is a required regulator for maintaining normal islet vasculature. Furthermore, β-cell–specific c-Kit overexpression (*c-KitβTg*) in aged mice showed significantly increased islet vasculature and β-cell function, but, when exposed to a long-term high-fat diet, c-Kit signaling in *c-KitβTg* mice induced substantial vascular remodeling, which resulted in increased islet inflammatory responses and β-cell apoptosis. These results suggest that c-Kit–mediated VEGF-A action in β-cells plays a pivotal role in maintaining islet vascularization and function.

The receptor tyrosine kinase c-Kit plays an important role in β-cell function and maturation (1–5). Mice with a heterozygous global mutation of c-Kit (*c-Kit*$^{Wv/+}$) demonstrated a severe loss of β-cell mass and impaired insulin release (6–8), whereas restoration of c-Kit expression specifically in β-cells of these mice resulted in increased β-cell mass and improved glucose tolerance (9). Increasing evidence suggests that c-Kit and its ligand, stem cell factor (SCF), are implicated in the regulation of angiogenesis. SCF treatment of different c-Kit–expressing neoplastic cell lines revealed a significant stimulatory effect on vascular endothelial growth factor (VEGF) secretion, which was inhibited by the tyrosine kinase inhibitor imatinib (10–12). Additionally, bone marrow stem cells/progenitor cells expressing c-Kit can establish a proangiogenic milieu by releasing VEGF (13,14), while a mutation resulting in loss of function in c-Kit in bone marrow stem cells/progenitor cells prevented angiogenesis by interfering with myocardial repair tissue formation (14).

Vascular innervation of islets is required for proper endocrine pancreatic organogenesis (15), mediated by VEGF isoform A (VEGF-A) production from β-cells (16–18). Prior studies (15,16,18), using a β-cell–specific VEGF-A–deficient mouse model, demonstrated that abnormally developed vasculature impairs islet architecture and glucose metabolism. In contrast, more recent reports (19,20) have demonstrated that β-cell–specific de novo induction of VEGF-A–stimulated endothelial cell (EC) activation is associated with a progressive loss in β-cell function and mass. Thus, further studies are required to examine the underlying mechanisms that regulate VEGF-A production in β-cells.

[1]Children's Health Research Institute, University of Western Ontario, London, Ontario, Canada
[2]Department of Physiology and Pharmacology, University of Western Ontario, London, Ontario, Canada
[3]Department of Pathology, University of Western Ontario, London, Ontario, Canada
[4]Genetics and Developmental Biology, University of Connecticut Health Center, Farmington, CT
[5]Department of Medicine, University of Western Ontario, London, Ontario, Canada

Corresponding author: Rennian Wang, rwang@uwo.ca.

Received 12 January 2015 and accepted 25 July 2015.

This article contains Supplementary Data online at http://diabetes.diabetesjournals.org/lookup/suppl/doi:10.2337/db15-0054/-/DC1.

The correlation between c-Kit and angiogenesis in different cell types has been established in previous research, yet whether c-Kit serves a primary role in regulating islet vascular remodeling by mediating VEGF-A production needs to be clarified. It is widely accepted that the vascular niche provides oxygen and exchanges nutrients and metabolites to support β-cell survival (18), but it can also expose islets to inflammatory mediators under abnormal metabolic conditions (20–22). Here, we aimed to investigate the role of c-Kit–mediated VEGF-A and islet vasculature and its impact on islet survival and function under normal physiological and pathological diabetic conditions using a combination of in vitro cell line and ex vivo islet cultures and different animal models. Our results showed that c-Kit is directly involved in islet vascularization and β-cell function through its signaling to modulate VEGF-A production in β-cells via the Akt/mammalian target of rapamycin (mTOR) axis. We further showed that *c-Kit*$^{Wv/+}$ mice with ablated c-Kit function had a substantial loss of β-cell mass and islet vasculature that was reversible by restoring c-Kit expression in the β-cells. On a normal diet, aged transgenic mice with a specific overexpression of c-Kit in β-cells (*c-KitβTg*) resulted in increased islet vascularization, which was correlated with β-cell expansion. Interestingly, aged *c-KitβTg* mice under long-term high-fat diet (HFD) feeding conditions showed islet hypervascularization and increased islet inflammatory responses resulting in β-cell dysfunction and apoptosis.

RESEARCH DESIGN AND METHODS

Animals

c-Kit$^{Wv/+}$ *and β-Cell–Specific c-Kit Overexpression in* c-Kit$^{Wv/+}$ *Mice at 8 Weeks of Age*

Heterozygous *c-Kit*$^{Wv/+}$ mice obtained from The Jackson Laboratory (stock #000049) (6) were crossbred with *c-KitβTg* mice to generate the following four experimental groups: wild-type (WT); *c-Kit*$^{Wv/+}$; *c-KitβTg*; and *c-KitβTg:c-Kit*$^{Wv/+}$ (*c-KitβTg:Wv*) (9). These mice were fed a normal diet, and pancreata were collected at 8 weeks for morphological analyses.

c-KitβTg *Mice at 28 Weeks of Age With Normal or HFD Studies*

c-KitβTg mice and their age-matched WT littermates were generated as described previously (9). An HFD study was performed using HFD (D12492; Research Diets, New Brunswick, NJ) for 20–22 weeks, starting at 6 weeks of age for both WT (*WT-HFD*) and *c-KitβTg* (*c-KitβTg-HFD*) mice (9). In parallel, age-matched WT and *c-KitβTg* mice under normal diet conditions were examined. Metabolic studies were performed at 28 weeks of age.

All mice were maintained on a C57BL/6J background. The *c-Kit*$^{Wv/+}$ mice were identified by their characteristic pigmentation, and the *c-KitβTg* mice were identified by PCR, as previously described (6,9). Female mice were excluded from this study. All animal work was performed under protocols approved by the Animal Use Subcommittee at the University of Western Ontario in accordance with the guidelines of the Canadian Council on Animal Care.

Metabolic Studies on Experimental Mouse Models

Metabolic studies on *c-KitβTg:Wv* mice with their aged-matched experimental littermates at 8 weeks of age were previously reported (9). Body weight and blood glucose levels were measured, and an intraperitoneal glucose tolerance test (IPGTT) and an intraperitoneal insulin tolerance test (IPITT) were performed on WT and *c-KitβTg* mice at 4, 10, 16, and 20–22 weeks post-HFD and at 28 weeks of age (9). For the IPGTT and IPITT, an intraperitoneal injection of glucose (D-(+)-glucose; Sigma-Aldrich, St. Louis, MO) at a dosage of 2 mg/g body weight or human insulin (Humalin; Eli Lilly, Toronto, ON, Canada) at 1 unit/kg body weight, respectively, was administered. Blood glucose levels were measured before and after injection, and the area under the curve (AUC) was used to quantify responsiveness.

INS-1 Cell and Ex Vivo Islet Cultures

INS-1 832/13 cells were cultured in RPMI 1640 medium containing 10% FBS (Invitrogen, Burlington, ON, Canada) (8). At 80% confluency, INS-1 cells were starved in serum-free RPMI 1640 medium containing 1% BSA overnight prior to the experiment. For SCF stimulation studies, cells were treated for 24 h with human recombinant SCF at 10–100 ng/mL (dissolved in acetic acid; ID Laboratories, London, ON, Canada) or cultured with SCF at 50 ng/mL for 1, 6, or 24 h; controls were treated with the same amount of SCF vehicle. For the *c-Kit* small interfering RNA (siRNA) studies, INS-1 cells were transiently transfected for 72 h with either *c-Kit*(r) siRNA (sc-36533) or control siRNA (sc-37007) followed by treatment with 50 ng/mL SCF or SCF vehicle for 24 h (8). For signaling inhibitory studies, INS-1 cells were pretreated with either Lys294002 (a PI3K inhibitor) at 1–100 μmol/L (dissolved in DMSO; Promega, Madison, WI) or rapamycin (an mTOR inhibitor) at 1–100 nmol/L (dissolved in DMSO; LC Laboratories, Woburn, MA) for 30 min, and then cultured with SCF (50 ng/mL) or SCF vehicle. Cells were processed for RNA or protein extraction or were fixed for immunocytochemistry studies, and culture media were collected for VEGF-A secretion analysis.

Primary islets were isolated from WT and *c-KitβTg* mice at 10 weeks of age and cultured in RPMI 1640 media plus 1% BSA with or without SCF (50 ng/mL) for 24 h. Islets were harvested for protein extraction, and culture media were collected for VEGF-A secretion analysis.

ELISA Assay for VEGF-A and Insulin

INS-1 cells and ex vivo islet culture media were harvested and analyzed with a Murine VEGF Mini ELISA Kit (Peprotech, Rocky Hill, NJ). For the in vivo glucose-stimulated insulin secretion (GSIS) assay, mouse plasma was collected following 4 h of fasting (0 min) and at 5 and 35 min after glucose loading. Insulin secretion was measured using an Mouse Ultrasensitive Insulin ELISA Kit (ALPCO, Salem, NH) (9).

Immunofluorescence and Morphometric Analyses

Mouse pancreata were fixed in 4% paraformaldehyde and embedded in paraffin. Sections were prepared and stained with primary antibodies at appropriate dilutions, which are provided in Supplementary Table 1. Images were captured using Image-Pro Plus software (Media Cybernetics, Rockville, MD). Quantitative evaluations of islet density, average islet and β-cell size, and total β-cell mass were performed as previously described (8,9). Endocrine compartment vasculature (islet capillary density, capillary area per islet, and average islet capillary size and diameter) and exocrine compartment vasculature (exocrine capillary density and area) were measured (18,21). Islet EC and β-cell proliferation, transcription factor expression, and macrophage infiltration were determined by double immunofluorescence or immunohistochemical staining (8,9). Cell apoptosis was quantified by $TUNEL^+$ labeling on $insulin^+$ cells. A minimum of 10–12 random islets per pancreatic section per experimental group were analyzed, with at least four pancreata per age per experimental group (8,9).

Protein Extraction and Western Blot Analysis

Proteins from INS-1 cells and mouse islets were extracted in an NP-40 lysis buffer. An equal amount of protein was fractionated by 7.5%, 10%, or 12% SDS-PAGE, transferred onto a nitrocellulose membrane (Bio-Rad Laboratories, Mississauga, ON). Membranes were incubated with the primary antibodies listed in Supplementary Table 1 (8,9). Proteins were detected using ECL-Plus Western Blot Detection Reagents (PerkinElmer, Waltham, MA) and imaged by the VersaDoc Imaging System (Bio-Rad Laboratories). Signal intensities were densitometrically quantified by Image Lab Software. Data were normalized to total or loading controls (8,9).

RNA Extraction and Real-Time PCR Analysis

Total RNA was extracted from INS-1 cells and mouse islets using the RNAqueous-4PCR Kit (Invitrogen) (6). Sequences of PCR primers are provided in Supplementary Table 2. Real-time PCR analyses were performed using the iQ SYBR Green Supermix kit (Bio-Rad Laboratories). Relative levels of gene expression were calculated and normalized to the internal standard, 18S rRNA. Controls were performed by omitting reverse transcriptase, cDNA, or DNA polymerase (8,9).

Statistical Analysis

Data are expressed as the mean ± SEM. Statistical significance was determined by paired or unpaired Student *t* test if comparing only two groups or one-way ANOVA followed by Fisher least significant differences (LSD) post hoc tests if analyzing more than two groups. Differences were considered to be statistically significant at $P < 0.05$.

RESULTS

c-Kit Signaling Regulates VEGF-A Production Via the Akt/mTOR Pathway in β-Cells

INS-1 832/13 cells were previously found to have high expression of c-Kit (5,8), and, under SCF stimulation, they displayed enhanced VEGF-A secretion in a dose- and time-dependent fashion (Fig. 1*A* and *B*) that is associated with increased phosphorylation of c-Kit (Fig. 1*E*). Cells treated with 50 ng/mL SCF for 24 h exhibited a threefold increase in hypoxia-inducible factor-1α (*HIF-1α*) and *VEGF-A* mRNA expression (Fig. 1*C*) and an ∼30% increase in VEGF-A protein levels when compared with controls (Fig. 1*D*). siRNA-mediated c-Kit knockdown significantly decreased SCF-stimulated c-Kit phosphorylation (Fig. 2*A*) and resulted in a downregulation of VEGF-A content and secretion (Fig. 2*B*). Ex vivo islets cultures showed that VEGF-A secretion from WT islets was not significantly induced after SCF stimulation, yet a higher level of VEGF-A secretion was observed in SCF-treated *c-KitβTg* islets (Supplementary Fig. 1*A*). VEGF-A protein levels were also significantly elevated in *c-KitβTg-SCF* islets compared with WT groups (Supplementary Fig. 1*B*), suggesting that c-Kit signaling mediates VEGF-A production in β-cells.

We further examined c-Kit downstream signaling molecules that are involved in regulating VEGF-A production. INS-1 cells treated with SCF showed significantly enhanced levels of phosphorylated (phospho)-Akt, without a change in mitogen-activated protein kinase activity (Fig. 1*E*), and was associated with an increase in mTOR phosphorylation and downstream targets P70S6K and NFκBp65 (Fig. 1*E*). SCF-mediated c-Kit receptor signaling changes were significantly reduced when cells were pretreated with *c-Kit* siRNA (Fig. 2*C*). Additionally, SCF failed to activate c-Kit–induced VEGF-A production in a dose-dependent manner in INS-1 cells pretreated with either Lys294002 (Fig. 1*F*) or rapamycin (Fig. 1*G*). These results verified that the PI3K/Akt/mTOR signaling pathway influences c-Kit–regulated VEGF-A production.

c-Kit Function Is Required for Maintaining Normal Islet Vasculature In Vivo

To directly investigate the islet vasculature, we performed immunostaining for platelet endothelial cell adhesion molecule 1 (PECAM-1), an EC-specific marker, in 8-week-old WT, *c-Kit*$^{Wv/+}$, *c-KitβTg*, and *c-KitβTg:Wv* mouse islets. Our results demonstrated reduced staining for $PECAM\text{-}1^+$ cells (Fig. 3*A*), but no substantial change in islet capillary density (Fig. 3*B*), in *c-Kit*$^{Wv/+}$ mouse islets compared with WT mouse islets. However, a significantly decreased blood vessel area relative to islet area (Fig. 3*B* and *C*), an ∼50% reduction in the average islet capillary size (Fig. 3*D*), and an ∼40% decrease in the internal capillary diameter (Fig. 3*E*) were found in *c-Kit*$^{Wv/+}$ mouse islets compared with the WT and *c-KitβTg* groups. In contrast with *c-Kit*$^{Wv/+}$ mice, there was significant improvement in capillary density and area (Fig. 3*B* and *C*), as well as a 40% increase in average capillary size (Fig. 3*D*) and islet capillary diameter (Fig. 3*E*), in both *c-KitβTg* and *c-KitβTg:Wv* mouse islets. Interestingly, islet vasculature morphologies were comparable among WT, *c-KitβTg*, and *c-KitβTg:Wv* mice at 8 weeks of age (Fig. 3*A*–*E*). These results demonstrate that c-Kit function is required for maintaining normal vasculature in mouse islets.

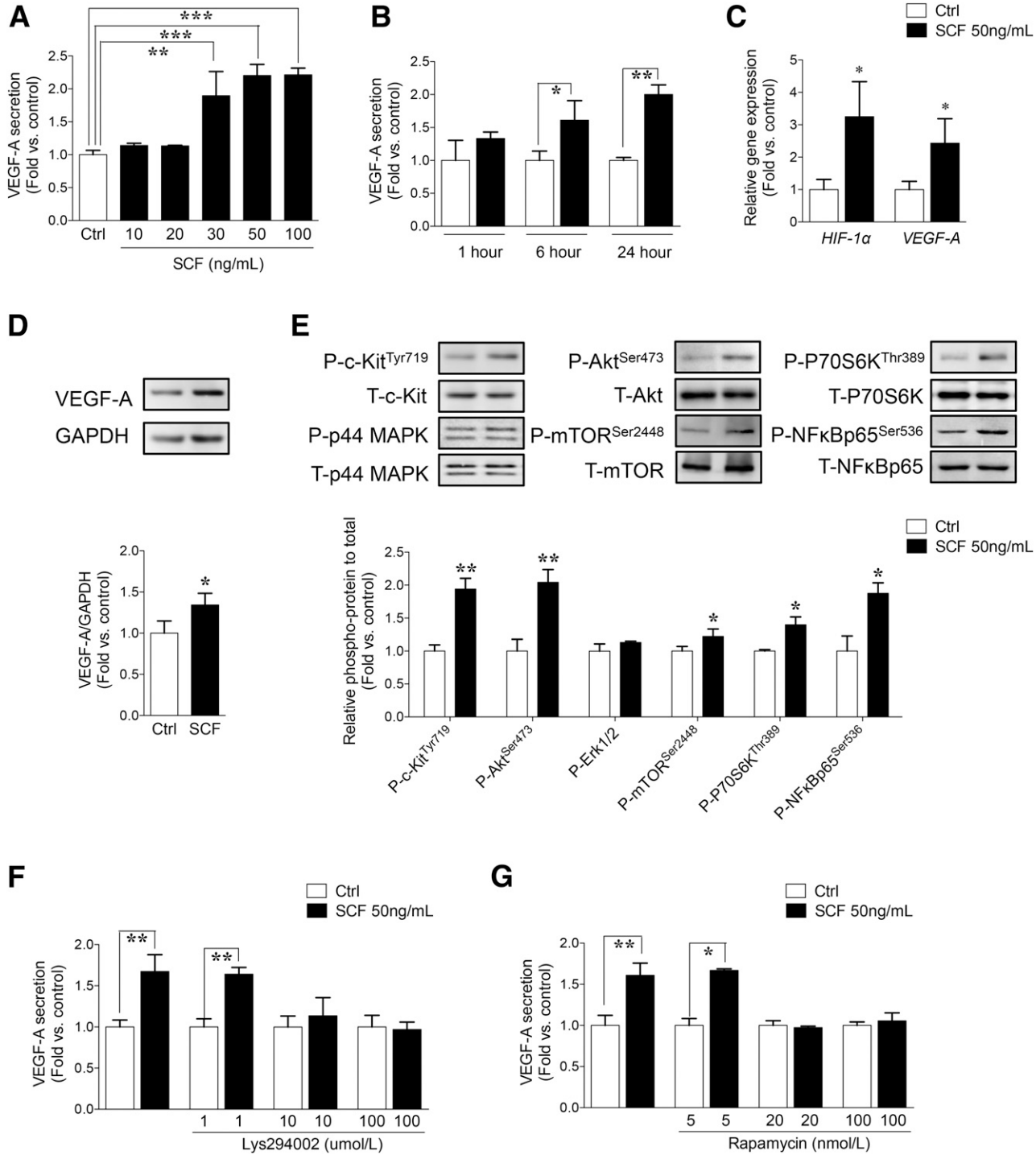

Figure 1— SCF-stimulated c-Kit signaling regulates VEGF-A production via the Akt/mTOR pathway in INS-1 cells. INS-1 cells were cultured in serum-free medium in the absence or presence of SCF for up to 24 h. Dose-dependent (*A*) and time-dependent (*B*) VEGF-A secretion were assayed by ELISA (N = 3–4 experiments/treatment group). Quantitative real-time PCR analyses of *HIF-1α* and *VEGF-A* mRNA (*C*), Western blot analyses of VEGF-A (*D*), and associated intracellular signaling molecules (*E*) in INS-1 cells following administration of 50 ng/mL SCF for 24 h. ELISA analyses of VEGF-A secretion from INS-1 cells cultured in serum-free medium in the presence of SCF compared with SCF plus PI3K inhibitor (Lys294002, 1–100 umol/L) (*F*) or SCF plus mTOR inhibitor (rapamycin, 5–100 nmol/L) (*G*) (N = 3 experiments/treatment group). Representative blots are shown. Data (*A*–*G*) are expressed as the mean ± SEM. $^{*}P < 0.05$, $^{**}P < 0.01$, $^{***}P < 0.001$, by paired Student t test or one-way ANOVA followed by Fisher LSD post hoc analyses if more than two groups (see also Supplementary Fig. 1). Ctrl, control; P, phospho; T, total.

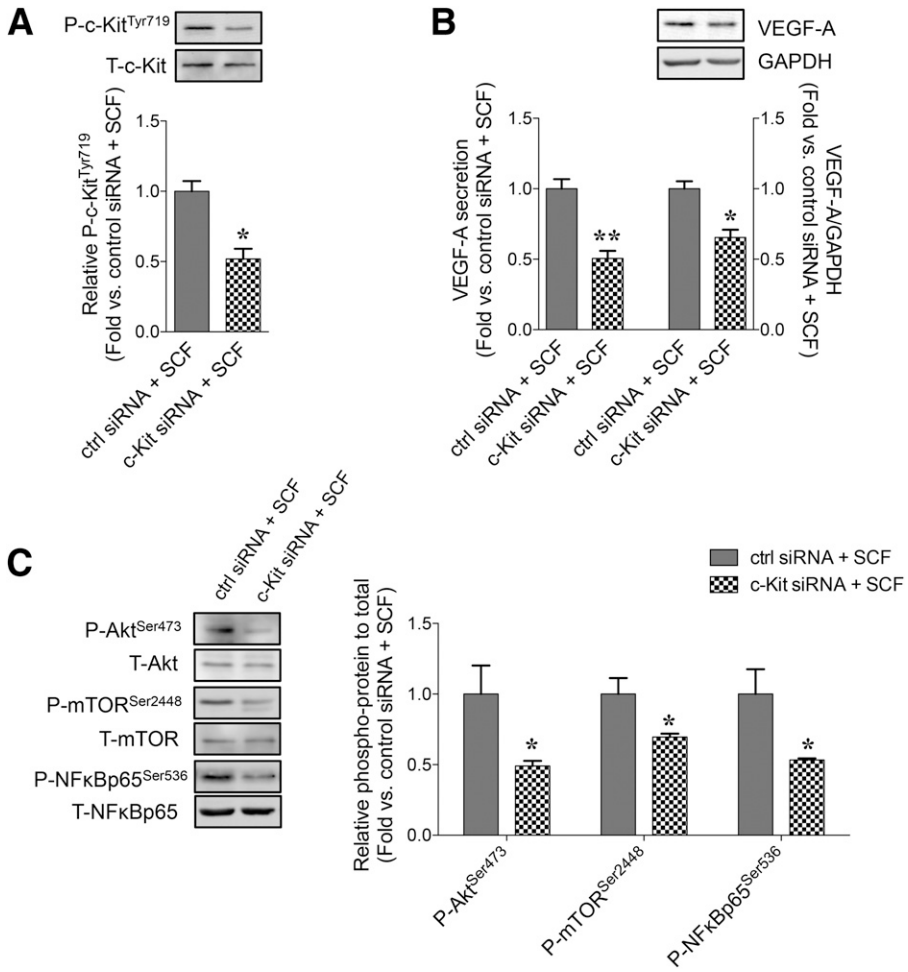

Figure 2—siRNA knockdown of c-Kit reduces SCF-stimulated c-Kit mediation of VEGF-A production through the Akt/mTOR pathway. Western blot analysis of phospho (P)-c-Kit^{Tyr719} expression (*A*), ELISA analysis of VEGF-A secretion and Western blot analysis of VEGF-A protein levels (*B*), and associated intracellular signaling molecules (*C*) from INS-1 cells transfected with control or *c-Kit* siRNA for 72 h plus SCF (50 ng/mL) for 24 h. Representative blots are shown. *A–C*: Data are expressed as the mean ± SEM (N = 3–4 experiments/treatment group). *$P < 0.05$, **$P < 0.01$ vs. control siRNA group, analyzed by paired Student *t* test. ctrl, control; T, total.

c-Kit Modulates Islet Vasculature Via the Akt/mTOR Pathway and VEGF-A Production In Vivo

In parallel to our INS-1 study, we examined whether the Akt/mTOR signaling pathway was involved in maintaining islet vasculature in vivo. In *c-Kit*$^{Wv/+}$ islets, we found significant decreases in the phosphorylation of Akt, P70S6K, and NFκBp65 (Fig. 3*F*), with an ~40% reduction in VEGF-A and an ~50% decline in Pdx-1 protein levels (Fig. 3*G*). Restoration of c-Kit expression in *c-Kit*$^{Wv/+}$ β-cells (*c-KitβTg:Wv*) restored the Akt/mTOR/NFκBp65 pathway and increased the levels of VEGF-A and Pdx-1 protein to levels similar to those of WT islets (Fig. 3*F* and *G*). Phospho-Akt was significantly increased in *c-KitβTg* islets (vs. WT islets; Fig. 3*F*), yet phosphorylation of P70S6K and NFκBp65 and associated VEGF-A levels were relatively unchanged (Fig. 3*F* and *G*), which is corroborated by only a marginal increase in islet vasculature in *c-KitβTg* mice at 8 weeks of age (Fig. 3*A–E*). Also, an observed reduction of Pdx-1, Nkx6.1, and MafA immunostaining in *c-Kit*$^{Wv/+}$ islets was reversed by restored c-Kit expression in *c-KitβTg:Wv* mice (Supplementary Fig. 2), supporting the fact that islet vasculature is important for islet transcription factor expression and function.

c-Kit Overexpression in β-Cells Increases Islet Vasculature, Islet Number, and β-Cell Proliferation

Islet vasculature in aged mice was examined to determine whether c-Kit–mediated vascularization is age dependent. At 28 weeks of age, *c-KitβTg* islets showed increased PECAM-1$^+$ staining (Fig. 4*A*), islet capillary density (Fig. 4*B*), and vessel area-to-islet area ratios (Fig. 4*C*), with a 1.6-fold increased islet EC proliferation (1.7 ± 0.2%) compared with WT groups (1.1 ± 0.3%). However, no changes in average capillary size or diameter in the islets (Fig. 4*D* and *E*) and no vascular alterations in exocrine pancreas were observed (Supplementary Fig. 3*A* and *B*). Increased islet capillary density was corroborated by a total increase of PECAM-1 protein levels and an ~40%

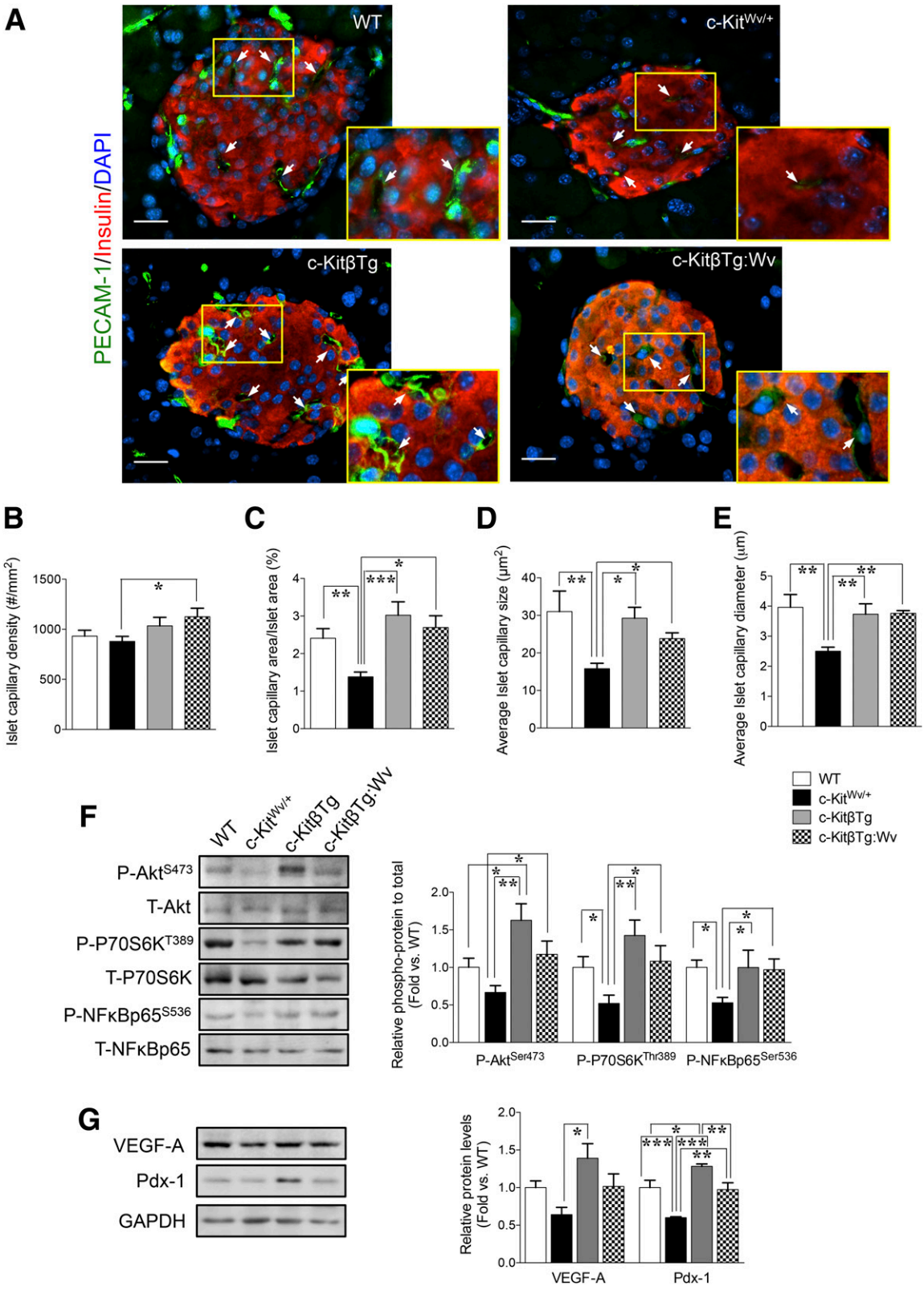

Figure 3—Overexpressing c-Kit in β-cells rescues the loss of islet vasculature in *c-Kit*$^{Wv/+}$ mice. *A*: Representative images of PECAM-1 (green) costained with insulin (red) and nuclear stain DAPI (blue) of 8-week-old male WT, *c-Kit*$^{Wv/+}$, *c-KitβTg*, and *c-KitβTg:Wv* pancreatic sections. Scale bar, 25 μm. Magnified images are shown in insets. Arrows, PECAM-1$^+$ cells in the islets. Quantitative analyses of islet capillary density (*B*), the ratio of islet capillary area to islet area (*C*), the average islet capillary size (*D*), and the average islet capillary diameter (*E*) in pancreatic sections from all experimental groups. Western blot analyses of phospho-Akt (P-Akt) and total Akt (T-Akt), phospho-P70S6K (P-P70S6K) and total P70S6K (T-P70S6K), phospho-NFκBp65 (P-NFκBp65) and total NFκBp65 (T-NFκBp65) (*F*), and VEGF-A and Pdx-1 protein expression (*G*) in islets isolated from 8-week-old male WT, *c-Kit*$^{Wv/+}$, *c-KitβTg*, and *c-KitβTg:Wv* mice.

increase in islet VEGF-A content in aged *c-KitβTg* islets (Fig. 4*F*). While increased vasculature was associated with islet expansion through increased islet density and size (Fig. 4*G* and *H*), no changes in average β-cell size were observed, but increased β-cell mass and proliferative capacity were found (Fig. 4*I–K*). The expression of islet transcriptional factors Pdx-1 and Nkx6.1 (Supplementary Fig. 3*C*) were relatively enhanced in aged *c-KitβTg* mice compared with WT mice. Additionally, aged *c-KitβTg* mice displayed improved overnight fasting blood glucose levels (Fig. 4*L*) and better glucose tolerance, as revealed by significant decreases in the AUC of IPGTT results (Fig. 4*M*); no changes in insulin tolerance were found (Supplementary Fig. 3*D*).

c-Kit Overexpression–Induced Hypervasculature Impairs β-Cell Function in Aged *c-KitβTg* Mice Under a Long-term HFD

On the basis of the results obtained from aged *c-KitβTg* mice under normal physiological conditions, we hypothesized that enhanced islet vascularization may protect islet survival and function under long-term (22 weeks) HFD-induced diabetic conditions. Immunostaining for PECAM-1 and insulin showed dilated capillaries with a greater accumulation of red blood cells in *c-KitβTg-HFD* islets (Fig. 5*A*). Although there were no changes in islet capillary density between the two experimental groups (Fig. 5*B*), there was a significant increase in the overall blood vessel area-to-islet area ratios (Fig. 5*C*), which was attributed to increased average islet capillary size (Fig. 5*D*) and intra-islet capillary diameter (Fig. 5*E*), in *c-KitβTg-HFD* islets. Increased islet EC proliferation was ~2.3-fold higher than that of *WT-HFD* (3 ± 1% vs. 1.3 ± 0.2%; Fig. 5*F*). The vasculature within pancreatic exocrine tissue remained unchanged between groups (Fig. 5*G* and *H*).

Although there were no significant differences in body, pancreas, or fat pad weights between *c-KitβTg-HFD* and *WT-HFD* littermates (Supplementary Fig. 4*A–C*), surprisingly, the overnight fasting blood glucose level was significantly higher in *c-KitβTg-HFD* mice (Fig. 6*A*). Glucose tolerance in *c-KitβTg-HFD* mice was progressively impaired, and there were significant increases in AUC when the IPGTT was performed after 20–22 weeks of HFD feeding (Fig. 6*B* and *C*). No significant changes in insulin tolerance were observed between groups (Supplementary Fig. 4*D*). In vivo GSIS assays showed significantly decreased plasma insulin levels at 35 min following glucose stimulation in *c-KitβTg-HFD* mice (Fig. 6*D*). The impaired glucose tolerance of *c-KitβTg-HFD* mice was associated with a significantly low number of islets (Fig. 6*E*). Although the average islet size was slightly increased (Fig. 6*F*), the average β-cell size was comparable while total β-cell mass was significantly decreased in HFD-fed *c-KitβTg* mice (Fig. 6*G* and *H*). No significant changes were observed in β-cell proliferation between the experimental groups (Fig. 6*I*). Notably, total E-cadherin protein levels in the islets (Fig. 6*J*) and the loss of E-cadherin expression on the β-cell surface (Fig. 6*K*) were displayed in *c-KitβTg-HFD* islets. Thus, the protective effects on glycemic control observed in *c-KitβTg* mice fed a normal chow diet were diminished after long-term HFD.

c-Kit Overexpression–Induced Hypervasculature Is Associated With Increased Islet Inflammatory Response in Aged *c-KitβTg* Mice Under a Long-term HFD

Higher levels of *VEGF-A* mRNA and protein were detected in *c-KitβTg-HFD* islets (Fig. 7*A* and *B*), while cleaved poly(ADP-ribose) polymerase protein levels were increased by ~45% (Fig. 7*C*), with a significant increase in the number of TUNEL$^+$ β-cells (Fig. 7*D*). Increased expression of Toll-like receptor 2 (TLR2) and inflammatory cytokine genes were further corroborated by Western blot analyses showing that protein levels of tumor necrosis factor-α (TNF-α), interleukin-1β (IL-1β), and Mac-2 were elevated in *c-KitβTg-HFD* islets (Fig. 7*E* and *F*). Increased macrophage infiltration in the islets was determined by Mac-2 immunohistochemistry (Fig. 7*G*), showing increased inflammatory responses in *c-KitβTg-HFD* islets. In contrast, those inflammatory cytokine genes were barely detectable, and few macrophage deposits were observed in the islets of mice fed a normal chow diet (Supplementary Fig. 5*A*), with no difference in Mac-2 protein levels between aged groups under normal diet feeding (Supplementary Fig. 5*B*).

DISCUSSION

The current study demonstrates that endocrine pancreatic c-Kit signaling is a critical regulator of islet vascular formation (Fig. 8*A*). Using the INS-1 cell line and ex vivo islet cultures, we showed that elevated c-Kit signaling increased VEGF-A production through upregulation of the downstream Akt/mTOR pathway. Using c-Kit mutation and overexpression mouse models, we observed impaired c-Kit signaling and reduced VEGF-A production that hampered normal islet vascular formation in *c-Kit*$^{Wv/+}$ mice, while the restoration of c-Kit signaling in β-cells of *c-Kit*$^{Wv/+}$ mice rescued vascular defects via signaling pathways identified in INS-1 cells. Sustained overexpression of c-Kit in β-cells not only increased islet vasculature but also led to improved glucose tolerance with enlarged β-cell mass in aged *c-KitβTg* mice. However, when *c-KitβTg* mice were subjected to a long-term HFD, they displayed substantial remodeling of islet vasculature, β-cell dysfunction and loss, and increased accumulation of inflammatory factors and macrophage infiltration in islets (Fig. 8*B*). Taken together, this study provides the first in vitro

Representative blots are shown (*N* = 4–5 animals/experimental group). *B–G*: Data are expressed as the mean ± SEM. $^*P < 0.05$, $^{**}P < 0.01$, $^{***}P < 0.001$, by one-way ANOVA followed by LSD post hoc analyses (see also Supplementary Fig. 2).

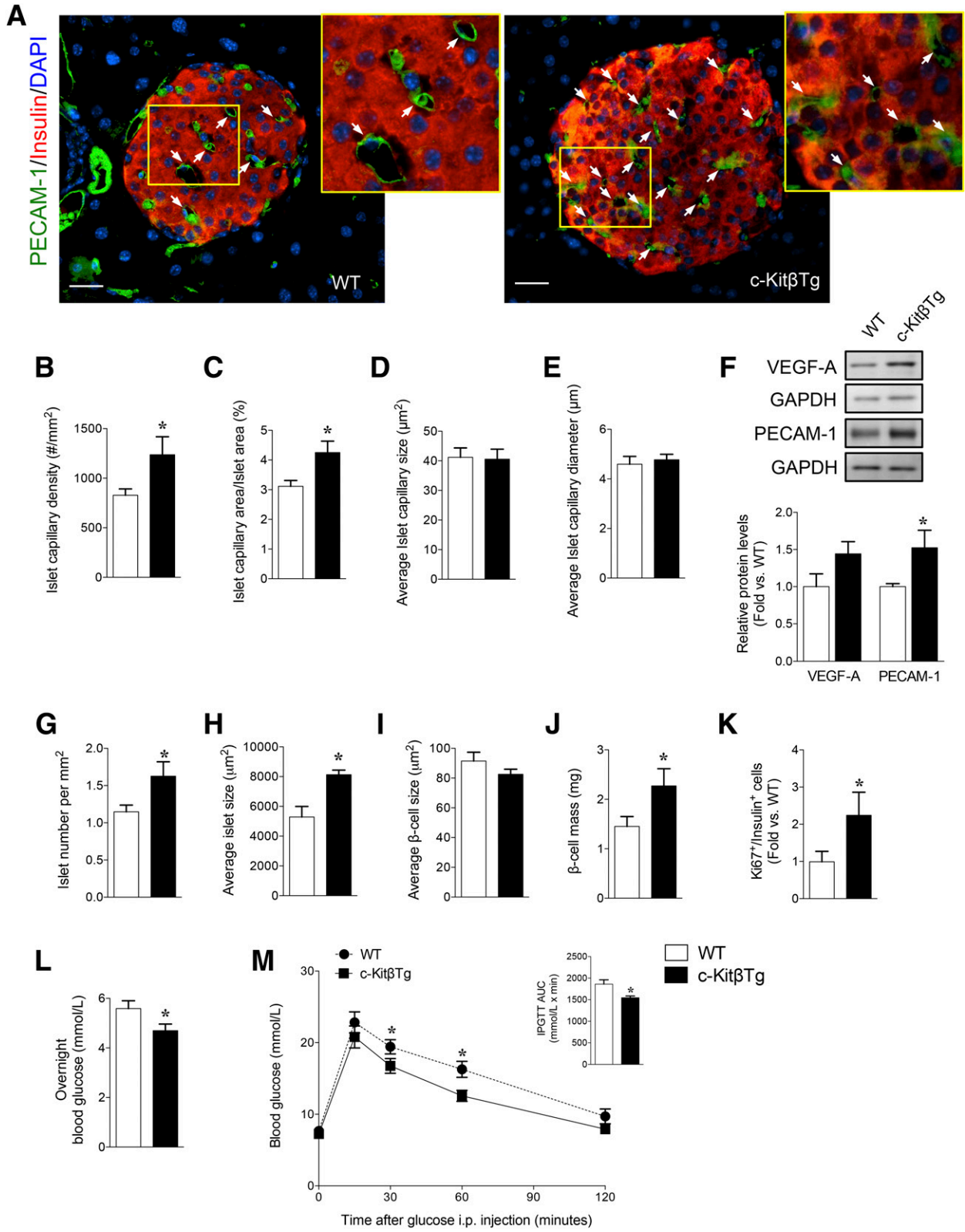

Figure 4—β-Cell–specific c-Kit overexpression increases islet vasculature and glucose metabolism in vivo. Islet vasculature and cellular morphology, as well as glucose tolerance, were analyzed in 28-week-old aged male WT and *c-KitβTg* mice. *A*: Representative images of PECAM-1 (green) costained with insulin (red) in aged WT and *c-KitβTg* mouse pancreatic sections. Nuclei were stained with DAPI (blue). Scale bar, 25 μm. Magnified images are shown in insets. Arrows, PECAM-1$^+$ cells in the islets. Quantitative analyses of islet capillary density (*B*), islet capillary area-to-islet area ratios (*C*), average islet capillary size (*D*) and diameter (*E*), and Western blot quantification of VEGF-A and PECAM-1 protein expression (*F*) in aged WT and c-*KitβTg* mouse islets. Islet number (*G*), average islet size (*H*), average β-cell size (*I*), total β-cell mass (*J*), Ki67$^+$ labeling of β-cells (*K*), overnight fasting blood glucose levels (*L*), and IPGTT results (*M*) were also analyzed in aged WT and *c-KitβTg* mice. *B–M*: Data are expressed as the mean ± SEM (N = 4–9 animals/experimental group). *$P < 0.05$, by unpaired Student t test (see also Supplementary Fig. 3).

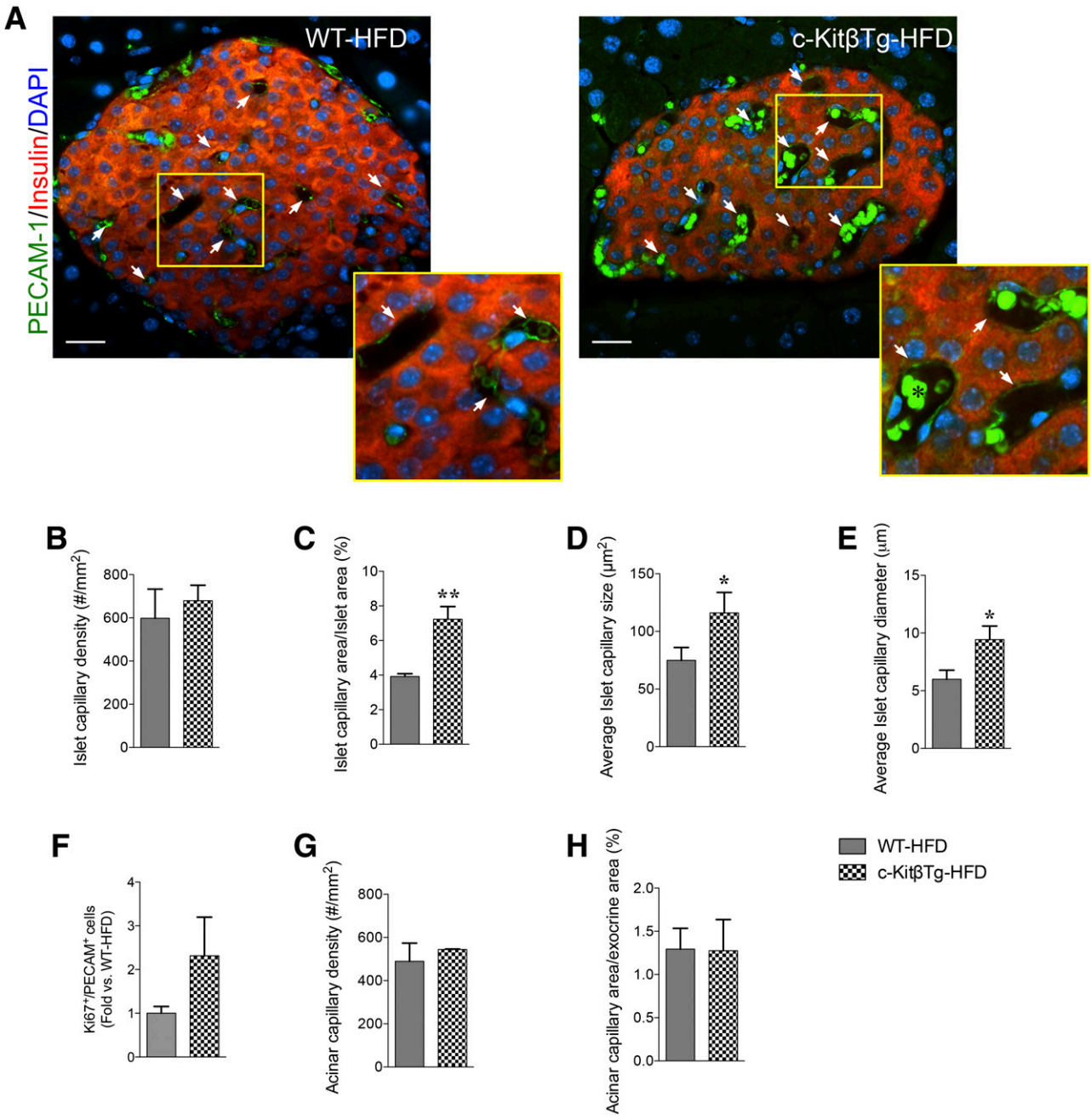

Figure 5—Increased vessel dilation in aged *c-KitβTg* mice under long-term HFD conditions. *A*: Representative images of PECAM-1 (green) costained with insulin (red) in 28-week-old *WT-HFD* and *c-KitβTg-HFD* mouse pancreatic sections. Scale bar, 25 μm. Magnified images are shown in insets. Arrows, PECAM-1$^+$ cells in the islets; asterisk, red blood cells. Quantitative analyses of vasculature and EC proliferation in endocrine (*B–F*) and exocrine (*G* and *H*) compartments in 28-week-old *WT-HFD* and *c-KitβTg-HFD* mice. *B–H*: Data are expressed as the mean ± SEM (N = 5 animals/experimental group). *$P < 0.05$, **$P < 0.01$, by unpaired Student t test.

and in vivo experiments to delineate the mechanism by which c-Kit–mediated VEGF-A production and islet vascular network modulate β-cell survival under normal and diabetic conditions.

c-Kit is highly expressed in the INS-1 insulinoma cell line, but its high expression levels in the pancreas are detected only during development and are reduced significantly in the postnatal pancreas, resulting in the low levels found in adult β-cells in humans and rodents (5,23,24). Using INS-1 cell culture, we demonstrated that SCF-stimulated c-Kit–mediated VEGF-A release was affected in both a dose- and time-dependent manner. Although we did observe stimulation in ex vivo cultures of primary islets isolated from WT mice, *c-KitβTg* mouse islets contained higher levels of c-Kit in β-cells that responded to 50 ng/mL SCF stimulation and led to significant increases in VEGF-A

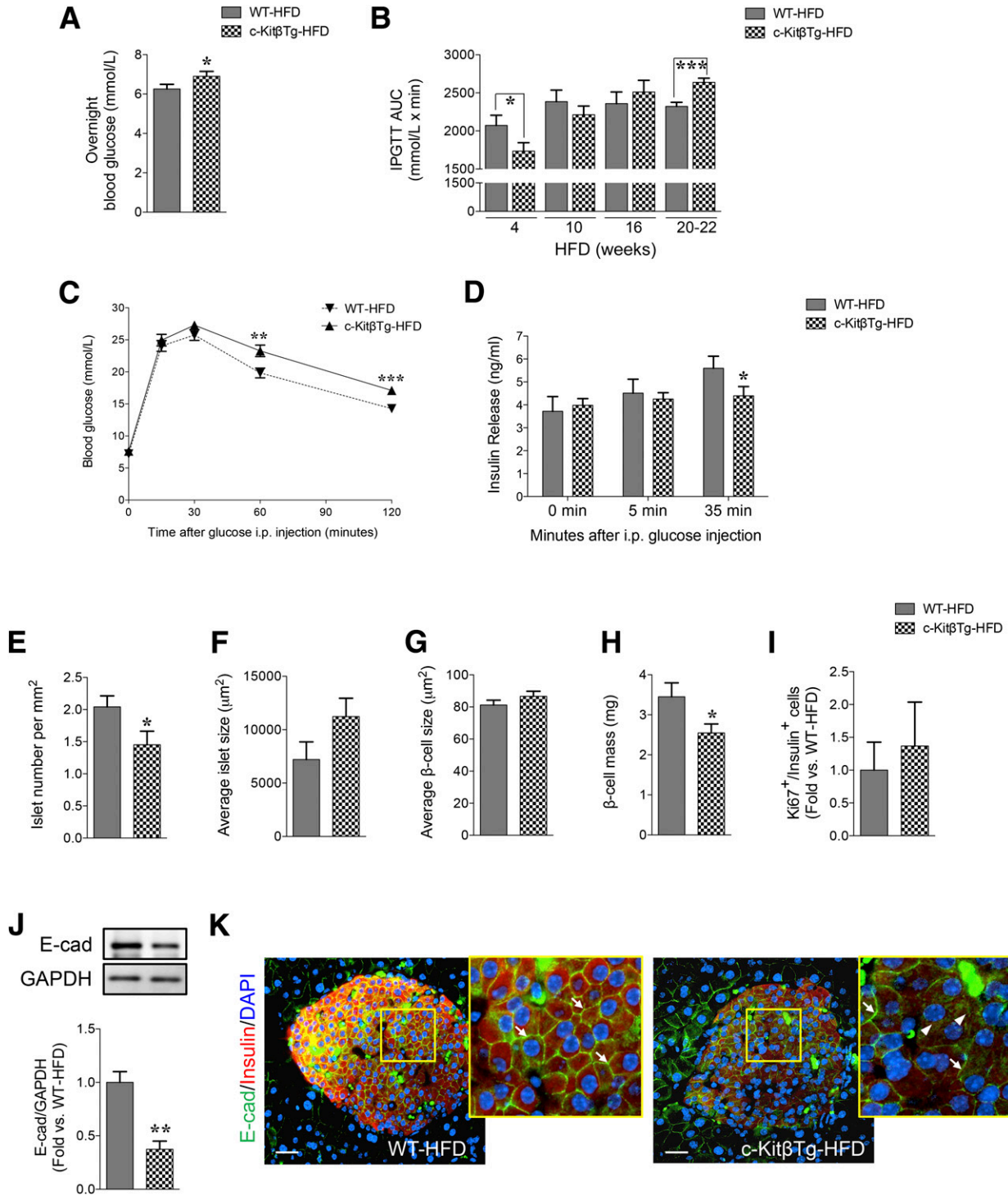

Figure 6—Islet hypervascularization results in impaired glucose tolerance in aged *c-KitβTg* mice under long-term HFD conditions. Overnight fasting blood glucose levels (*A*), measurement of IPGTT AUC after 4, 10, 16, and 20–22 weeks of being fed an HFD (*B*), and IPGTT results at 20 weeks of being fed an HFD (*C*) performed in *WT-HFD* and *c-KitβTg-HFD* mice. *D*: In vivo GSIS of *WT-HFD* and *c-KitβTg-HFD* mice. Quantitative analyses of islet number (*E*), average islet size (*F*), average β-cell size (*G*), total β-cell mass (*H*), and Ki67$^+$ labeling of β-cells (*I*) in *WT-HFD* and *c-KitβTg-HFD* mice. Western blot analysis of E-cadherin (E-cad) in isolated *WT-HFD* and *c-KitβTg-HFD* islets (*J*) and representative images of E-cadherin (green) costained with insulin (red) in *WT-HFD* and *c-KitβTg-HFD* mouse pancreatic sections (*K*). Scale bar, 25 μm. Magnified images are shown in insets. Arrows, the distribution of E-cadherin in the islets; arrowheads, the loss of E-cadherin in the β-cells. *A–J*: Data are expressed as the mean ± SEM (*N* = 4–5 animals/experimental group). **P* < 0.05, ***P* < 0.01, ****P* < 0.001, by unpaired Student *t* test (see also Supplementary Fig. 4).

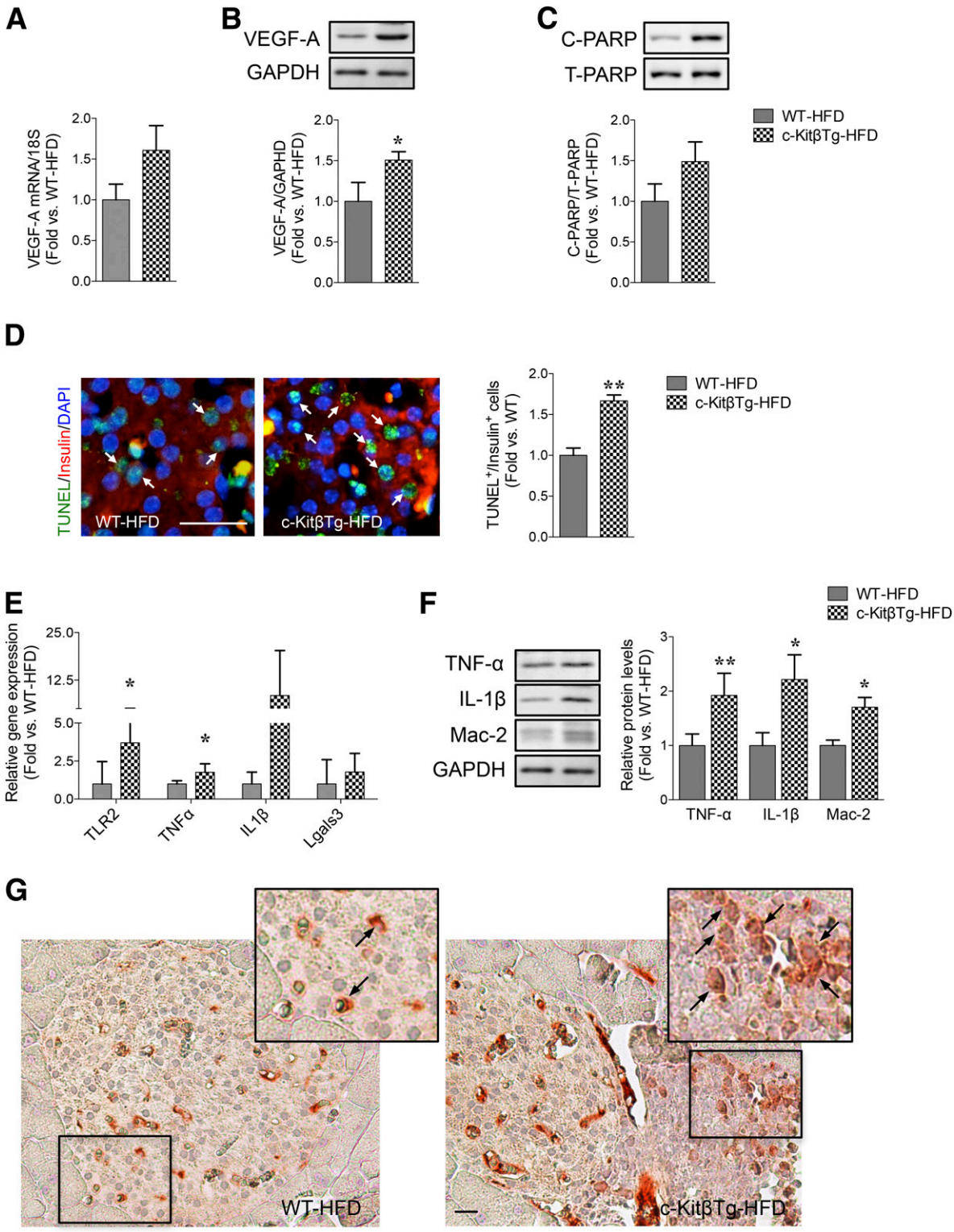

Figure 7— Islet hypervascularization results in increased numbers of inflammatory cytokines and macrophage infiltration in aged *c-KitβTg* mice under long-term HFD conditions. VEGF-A mRNA (*A*) and protein (*B*) and cleaved poly(ADP-ribose) polymerase (C-PARP) (*C*) in islets isolated from *WT-HFD* and *c-KitβTg-HFD* mice. *D*: Representative images of TUNEL (green) costained with insulin (red) and quantitative analysis of TUNEL$^+$/insulin$^+$ cells in *WT-HFD* and *c-KitβTg-HFD* mouse pancreatic sections. Scale bar, 25 μm. Arrows indicate TUNEL$^+$ nuclei. Quantitative real-time PCR analyses of selective inflammatory cytokine mRNA levels (*E*) and Western blot for TNF-α, IL-1β, and Mac-2 protein expressions (*F*) in islets isolated from *WT-HFD* and *c-KitβTg-HFD* mice. *G*: Immunohistochemical staining for Mac-2 (red) in *WT-HFD* and *c-KitβTg-HFD* mouse pancreatic sections. Scale bar, 25 μm. Arrows indicate Mac-2$^+$ cells. *A–F*: Data are expressed as the mean ± SEM (*N* = 3–5 animals/experimental group). **P* < 0.05, ***P* < 0.01, by unpaired Student *t* test (see also Supplementary Fig. 5). T, total.

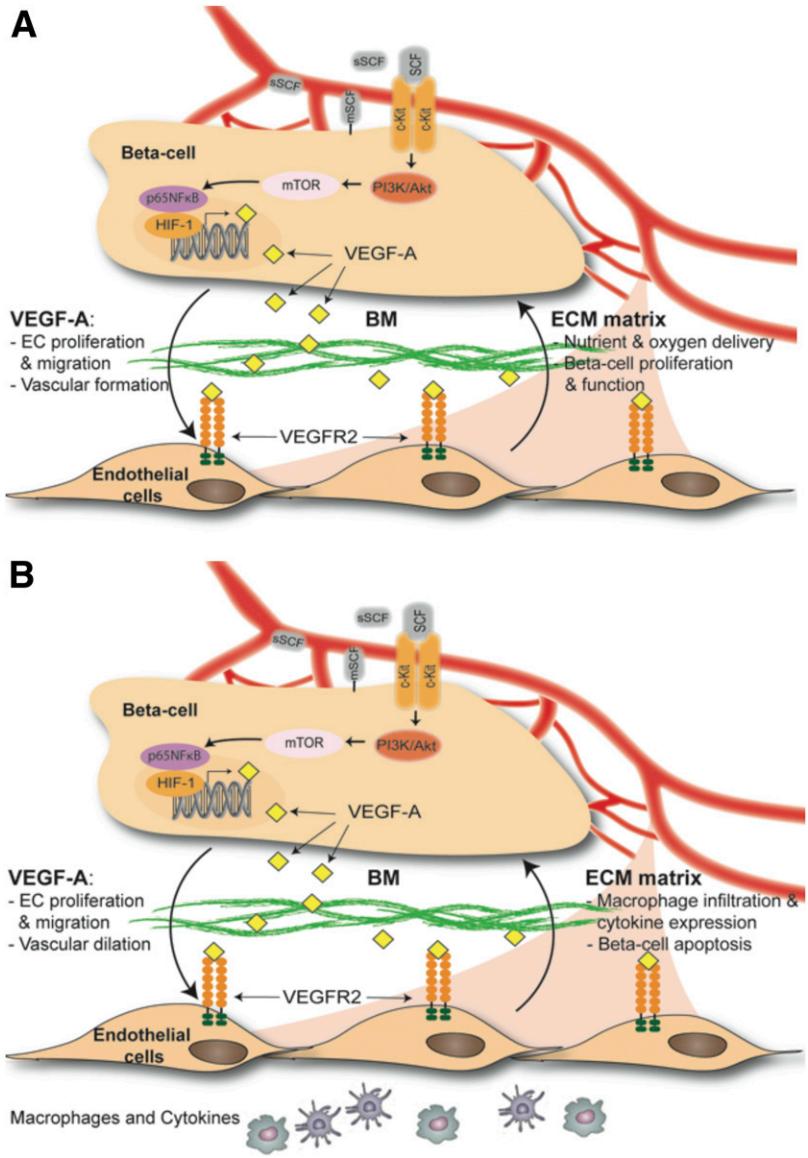

Figure 8—Proposed model of c-Kit signaling that mediates VEGF-A production and modulates islet vasculature, affecting β-cell function and survival. *A*: c-Kit mediates VEGF-A production via the PI3K/Akt/mTOR signaling, which is essential for maintaining islet vascular formation. Proper islet vasculature facilitates the nutrient and oxygen exchange that preserves β-cell survival and function. *B*: Chronic constitutive c-Kit–mediated VEGF-A overproduction results in increased islet vasculature. Under long-term HFD conditions, islets become hypervascularized, with increased cytokine production, macrophage infiltration, β-cell dysfunction, and apoptosis. BM, basement membrane; ECM, extracellular matrix; VEGFR2, VEGF receptor 2.

secretion and content. This indicates that a functional level of c-Kit expression in β-cells is essential for the response to SCF stimulation in mediating VEGF-A production. These studies suggest that c-Kit signaling is rate limiting but mediates VEGF-A production in β-cells.

The molecular mechanisms by which c-Kit regulates VEGF-A production in β-cells involve increased Akt/mTOR pathway activation and subsequent NFκBp65 and HIF-1α expression without signaling through mitogen-activated protein kinase. These mechanisms are consistent with studies showing that Akt-dependent regulation of NFκBp65 in HeLa cells can be controlled by mTOR (25) and that NFκBp65 binds to the HIF-1α promoter in neoplastic cell lines to modulate HIF-1α expression (26,27). Conversely, blockade of the NFκBp65 pathway in human primary hepatocellular carcinoma cells and murine peritoneal macrophages suppresses HIF-1α activity and results in decreased VEGF-A production (28,29). These results suggest that c-Kit activation of the Akt/mTOR pathway plays a critical role in VEGF-A production in multiple cell types, including β-cells, as revealed in the current study.

The relationship between c-Kit signaling and islet vascular formation was further defined in vivo. A substantial loss of islet vascularization was observed in

c-Kit$^{Wv/+}$ mice and rescued in *c-KitβTg:Wv* mice, demonstrating that β-cell–specific c-Kit signaling plays a critical role in the regulation of VEGF-A production and maintenance of islet vasculature. Proper islet capillary structure is critical to β-cell function and survival as it regulates the flow of nutrients and metabolites into islets, and proper fenestrations are required for insulin exocytosis into the bloodstream (Fig. 8*A*) (30,31). Our in vivo observations supported this hypothesis and showed increased islet vasculature in aged *c-KitβTg* mice with increased β-cell health and improved glucose tolerance. Taken together, the present findings demonstrate that β-cell–produced VEGF-A modulates the islet microenvironment and plays an important role in β-cell survival and function in mice.

HFD-fed *c-KitβTg* mice displayed impaired glucose tolerance and β-cell dysfunction alongside changes in the islet morphology, including hypervascularization, enlarged vascular size and diameter, and increased average islet size, but had reduced total β-cell mass. Given that the average β-cell size and proliferation were similar between experimental groups, we proposed that the loss of β-cell mass in *c-KitβTg-HFD* mice was due to islet hypervascularization associated with significantly increased inflammation and induced β-cell apoptosis. High levels of proinflammatory mediators (IL-1β and TNF-α) and macrophage infiltration were found in *c-KitβTg-HFD* islets, suggesting that islet inflammation might originate from endothelial activation. Previous studies (20,32,33) have shown that *VEGF-A* overexpression in β-cells leads to islet vascular abnormalities and impaired islet morphogenesis and function. Sustained overexpression of VEGF-A in the islets showed increased macrophage accumulation, collagen deposition, and expression of proinflammatory mediators (20), which could further promote β-cells to produce intracellular cytokines (34). Significantly increased TLR2 expression, linked to free fatty acid–induced inflammation, and the promotion of inflammatory cytokines (35), which was also observed in *c-KitβTg-HFD* mouse islets, could further recruit macrophages that perpetuate inflammatory processes within the islets and lead to eventual β-cell dysfunction. A previous study on TLR2-deficient mice (36) demonstrated that this model could be protected from islet inflammation and β-cell dysfunction in response to HFD feeding. Taken together, our observations of increased islet vascular dilation, hemorrhaging, and islet inflammation in *c-KitβTg-HFD* mice corroborate previous findings, suggesting that endothelial overactivation contributed to cytokine accumulation and macrophage deposition within islets of obesity-associated diabetic mice (20,21,34,37,38). More importantly, our findings demonstrated that the overstimulatory effect of c-Kit signaling on islet hypervasculature augments the inflammatory cycle and exacerbates β-cell death and dysfunction under the long-term HFD condition (Fig. 8*B*).

Notably, the observed glucose intolerance was associated with reduced in vivo insulin release, which was related to the loss of the cell-cell adhesion molecule E-cadherin in β-cells. E-cadherin is important for cell adhesion, forming adherens junctions that bind endocrine cells within islet clusters. Recent studies (39) indicated that the treatment of β-cells with an anti–E-cadherin blocking antibody affected intracellular Ca^{2+} levels and insulin secretion. Furthermore, the downregulation of E-cadherin in β-cells can induce a secretory defect and glucose intolerance (40–42). The interrelationship between E-cadherin and inflammatory cytokines has also been documented, where interferon-γ–treated, human colon–derived T84 epithelial cells led to a loss of membranous E-cadherin (43) and membrane-bound E-cadherin of prostatic cancer cells was disrupted during acute TNF-α exposure (44). These findings suggest that inflammatory cytokines influence membrane-localized E-cadherin, resulting in a loss of contact between cells and subsequent β-cell dysfunction in a long-term HFD setting.

In summary, our cell culture studies demonstrated that c-Kit regulation of VEGF-A production in β-cells via the Akt/mTOR/NFκBp65/HIF-1α pathway influences islet vasculature. Moreover, we found that β-cell–specific c-Kit overexpression in vivo promoted islet vasculature in aged *c-KitβTg* mice with enhanced β-cell function. Unexpectedly, aged *c-KitβTg* mice under long-term HFD conditions displayed vascular dilation associated with β-cell loss and dysfunction, intraislet infiltration of macrophages, increased levels of inflammatory cytokines, and hyperglycemia, all of which are hallmarks of non–insulin-dependent diabetes (45). The current study represents an integrated in vitro and in vivo approach to unraveling the cellular mechanisms by which c-Kit receptor signaling modulates VEGF-A production, vascularization, and β-cell function and suggests that c-Kit can be a potential therapeutic target in promoting revascularization in islet cell replacement therapy. Additionally, tight regulation of c-Kit activity is critical for the control of intraislet VEGF-A concentrations in order to maintain a normal islet vascular network for proper β-cell function and survival.

Acknowledgments. The authors thank Dr. Cindy Goodyer from McGill University for critically reading the manuscript and suggesting substantial improvements.

Funding. This work was supported by the Canadian Institutes of Health Research (grant MOP 89800). Z.-C.F. is a recipient of a Canadian Diabetes Association Doctoral Student Research Award.

Duality of Interest. No potential conflicts of interest relevant to this article were reported.

Author Contributions. Z.-C.F. and J.L. contributed to the acquisition, analysis, additional analysis, and interpretation of the data and the drafting, revision, and final approval of the article. A.P. and J.S. contributed to the acquisition, analysis, and interpretation of the data and the drafting and final approval of the article. A.O. contributed to additional data analysis, revision of the article, and final approval of the article. S.-P.Y. contributed to the provision of study materials, interpretation of the data, and revision and final approval of the article. R.W. contributed to the conception and design of the study; the collection, assembly, analysis, and interpretation of the data; and the drafting, revision, and final approval of the article. R.W. is the guarantor of this work and, as such, had full access to all the data in

the study and takes responsibility for the integrity of the data and the accuracy of the data analysis.

References

1. Feng Z-C, Riopel M, Popell A, Wang R. A survival kit for pancreatic beta cells: stem cell factor and c-Kit receptor tyrosine kinase. Diabetologia 2015;58: 654–665
2. Oberg C, Waltenberger J, Claesson-Welsh L, Welsh M. Expression of protein tyrosine kinases in islet cells: possible role of the Flk-1 receptor for beta-cell maturation from duct cells. Growth Factors 1994;10:115–126
3. Oberg-Welsh C, Welsh M. Effects of certain growth factors on in vitro maturation of rat fetal islet-like structures. Pancreas 1996;12:334–339
4. Welsh M, Annerén C, Lindholm C, Kriz V, Oberg-Welsh C. Role of tyrosine kinase signaling for beta-cell replication and survival. Ups J Med Sci 2000;105:7–15
5. Rachdi L, El Ghazi L, Bernex F, Panthier JJ, Czernichow P, Scharfmann R. Expression of the receptor tyrosine kinase KIT in mature β-cells and in the pancreas in development. Diabetes 2001;50:2021–2028
6. Krishnamurthy M, Ayazi F, Li J, et al. c-Kit in early onset of diabetes: a morphological and functional analysis of pancreatic beta-cells in c-KitW-v mutant mice. Endocrinology 2007;148:5520–5530
7. Feng Z-C, Donnelly L, Li J, Krishnamurthy M, Riopel M, Wang R. Inhibition of Gsk3β activity improves β-cell function in c-KitWv/+ male mice. Lab Invest 2012;92:543–555
8. Feng Z-C, Riopel M, Li J, Donnelly L, Wang R. Downregulation of Fas activity rescues early onset of diabetes in c-Kit(Wv/+) mice. Am J Physiol Endocrinol Metab 2013;304:E557–E565
9. Feng ZC, Li J, Turco BA, Riopel M, Yee SP, Wang R. Critical role of c-Kit in beta cell function: increased insulin secretion and protection against diabetes in a mouse model. Diabetologia 2012;55:2214–2225
10. Beppu K, Jaboine J, Merchant MS, Mackall CL, Thiele CJ. Effect of imatinib mesylate on neuroblastoma tumorigenesis and vascular endothelial growth factor expression. J Natl Cancer Inst 2004;96:46–55
11. Litz J, Sakuntala Warshamana-Greene G, Sulanke G, Lipson KE, Krystal GW. The multi-targeted kinase inhibitor SU5416 inhibits small cell lung cancer growth and angiogenesis, in part by blocking Kit-mediated VEGF expression. Lung Cancer 2004;46:283–291
12. Litz J, Krystal GW. Imatinib inhibits c-Kit-induced hypoxia-inducible factor-1alpha activity and vascular endothelial growth factor expression in small cell lung cancer cells. Mol Cancer Ther 2006;5:1415–1422
13. Li T-S, Hamano K, Nishida M, et al. CD117+ stem cells play a key role in therapeutic angiogenesis induced by bone marrow cell implantation. Am J Physiol Heart Circ Physiol 2003;285:H931–H937
14. Fazel S, Cimini M, Chen L, et al. Cardioprotective c-kit+ cells are from the bone marrow and regulate the myocardial balance of angiogenic cytokines. J Clin Invest 2006;116:1865–1877
15. Lammert E, Cleaver O, Melton D. Induction of pancreatic differentiation by signals from blood vessels. Science 2001;294:564–567
16. Lammert E, Gu G, McLaughlin M, et al. Role of VEGF-A in vascularization of pancreatic islets. Curr Biol 2003;13:1070–1074
17. Lai Y, Schneider D, Kidszun A, et al. Vascular endothelial growth factor increases functional beta-cell mass by improvement of angiogenesis of isolated human and murine pancreatic islets. Transplantation 2005;79:1530–1536
18. Brissova M, Shostak A, Shiota M, et al. Pancreatic islet production of vascular endothelial growth factor-A is essential for islet vascularization, revascularization, and function. Diabetes 2006;55:2974–2985
19. Iwashita N, Uchida T, Choi JB, et al. Impaired insulin secretion in vivo but enhanced insulin secretion from isolated islets in pancreatic beta cell-specific vascular endothelial growth factor-A knock-out mice. Diabetologia 2007;50:380–389
20. Agudo J, Ayuso E, Jimenez V, et al. Vascular endothelial growth factor–mediated islet hypervascularization and inflammation contribute to progressive reduction of β-cell mass. Diabetes 2012;61:2851–2861
21. Dai C, Brissova M, Reinert RB, et al. Pancreatic islet vasculature adapts to insulin resistance through dilation and not angiogenesis. Diabetes 2013;62:4144–4153
22. Ullsten S, Lau J, Carlsson P-O. Vascular heterogeneity between native rat pancreatic islets is responsible for differences in survival and revascularisation post transplantation. Diabetologia 2015;58:132–139
23. Yashpal NK, Li J, Wang R. Characterization of c-Kit and nestin expression during islet cell development in the prenatal and postnatal rat pancreas. Dev Dyn 2004;229:813–825
24. Li J, Quirt J, Do HQ, et al. Expression of c-Kit receptor tyrosine kinase and effect on beta-cell development in the human fetal pancreas. Am J Physiol Endocrinol Metab 2007;293:E475–E483
25. Dan HC, Cooper MJ, Cogswell PC, Duncan JA, Ting JP-Y, Baldwin AS. Akt-dependent regulation of NF-kappaB is controlled by mTOR and Raptor in association with IKK. Genes Dev 2008;22:1490–1500
26. Jung YJ, Isaacs JS, Lee S, Trepel J, Neckers L. IL-1beta-mediated up-regulation of HIF-1alpha via an NFkappaB/COX-2 pathway identifies HIF-1 as a critical link between inflammation and oncogenesis. FASEB J 2003;17:2115–2117
27. Ahmed M, Kundu GC. Osteopontin selectively regulates p70S6K/mTOR phosphorylation leading to NF-kappaB dependent AP-1-mediated ICAM-1 expression in breast cancer cells. Mol Cancer 2010;9:101
28. Figueroa YG, Chan AK, Ibrahim R, et al. NF-kappaB plays a key role in hypoxia-inducible factor-1-regulated erythropoietin gene expression. Exp Hematol 2002;30:1419–1427
29. Ramanathan M, Pinhal-Enfield G, Hao I, Leibovich SJ. Synergistic up-regulation of vascular endothelial growth factor (VEGF) expression in macrophages by adenosine A2A receptor agonists and endotoxin involves transcriptional regulation via the hypoxia response element in the VEGF promoter. Mol Biol Cell 2007; 18:14–23
30. Konstantinova I, Lammert E. Microvascular development: learning from pancreatic islets. Bioessays 2004;26:1069–1075
31. Richards OC, Raines SM, Attie AD. The role of blood vessels, endothelial cells, and vascular pericytes in insulin secretion and peripheral insulin action. Endocr Rev 2010;31:343–363
32. Cai Q, Brissova M, Reinert RB, et al. Enhanced expression of VEGF-A in β cells increases endothelial cell number but impairs islet morphogenesis and β cell proliferation. Dev Biol 2012;367:40–54
33. Brissova M, Aamodt K, Brahmachary P, et al. Islet microenvironment, modulated by vascular endothelial growth factor-A signaling, promotes β cell regeneration. Cell Metab 2014;19:498–511
34. Donath MY, Størling J, Berchtold LA, Billestrup N, Mandrup-Poulsen T. Cytokines and beta-cell biology: from concept to clinical translation. Endocr Rev 2008;29:334–350
35. Nguyen MTA, Favelyukis S, Nguyen A-K, et al. A subpopulation of macrophages infiltrates hypertrophic adipose tissue and is activated by free fatty acids via Toll-like receptors 2 and 4 and JNK-dependent pathways. J Biol Chem 2007; 282:35279–35292
36. Ehses JA, Perren A, Eppler E, et al. Increased number of islet-associated macrophages in type 2 diabetes. Diabetes 2007;56:2356–2370
37. Li X, Zhang L, Meshinchi S, et al. Islet microvasculature in islet hyperplasia and failure in a model of type 2 diabetes. Diabetes 2006;55:2965–2973
38. Tetè S, Tripodi D, Rosati M, et al. Endothelial cells, cholesterol, cytokines, and aging. Int J Immunopathol Pharmacol 2012;25:355–363
39. Rogers GJ, Hodgkin MN, Squires PE. E-cadherin and cell adhesion: a role in architecture and function in the pancreatic islet. Cell Physiol Biochem 2007;20: 987–994
40. Yamagata K, Nammo T, Moriwaki M, et al. Overexpression of dominant-negative mutant hepatocyte nuclear factor-1 α in pancreatic β-cells causes abnormal islet architecture with decreased expression of E-cadherin, reduced β-cell proliferation, and diabetes. Diabetes 2002;51:114–123
41. Jaques F, Jousset H, Tomas A, et al. Dual effect of cell-cell contact disruption on cytosolic calcium and insulin secretion. Endocrinology 2008;149: 2494–2505

42. Wakae-Takada N, Xuan S, Watanabe K, Meda P, Leibel RL. Molecular basis for the regulation of islet beta cell mass in mice: the role of E-cadherin. Diabetologia 2013;56:856–866
43. Smyth D, Leung G, Fernando M, McKay DM. Reduced surface expression of epithelial E-cadherin evoked by interferon-gamma is Fyn kinase-dependent. PLoS One 2012;7:e38441
44. Debelec-Butuner B, Alapinar C, Ertunc N, Gonen-Korkmaz C, Yörükoğlu K, Korkmaz KS. TNFα-mediated loss of β-catenin/E-cadherin association and subsequent increase in cell migration is partially restored by NKX3.1 expression in prostate cells. PLoS One 2014;9:e109868
45. Olefsky JM, Glass CK. Macrophages, inflammation, and insulin resistance. Annu Rev Physiol 2010;72:219–246